Trees (2014) 28:517–529
DOI 10.1007/s00468-013-0968-8

ORIGINAL PAPER

Loss in moment capacity of tree stems induced by decay

Cihan Ciftci · Brian Kane · Sergio F. Brena · Sanjay R. Arwade

Received: 7 August 2013 / Revised: 23 November 2013 / Accepted: 12 December 2013 / Published online: 29 December 2013

Abstract
Key message **We model varying decay in tree cross-sections by considering bending theory to estimate moment capacity loss (MCL) for the sections. We compare MCL with experiments on selected oak trees.**
Abstract Tree failures can damage property and injure people, sometimes with fatal consequences. Arborists assess the likelihood of failure by examining many factors, including strength loss in the stem or branch due to decay. Current methods for assessing strength loss due to decay are limited by not accounting for offset areas of decay and assuming that the neutral axis of the cross-section corresponds to the centroidal axis. This paper considers that strength loss of a tree can be related to moment capacity loss (MCL) of the decayed tree cross-section, because tree failures are assumed to occur when induced moments exceed the moment capacity of the tree cross-section. An estimation of MCL is theoretically derived to account for offset areas of decay and for differences in properties of wood under compressive and tensile stresses. Field measurements are used to validate the theoretical approach, and predictions of loss in moment capacity are plotted for a range of scenarios of decayed stems or branches. Results show that the location and size of decay in the cross-section and relative to the direction of sway are important to determine MCL. The effect of wood properties on MCL was most evident for concentric decay and decreased as the location of decay moved to the periphery of the stem. The effect of the ratio of tensile to compressive moduli of elasticity on calculations of MCL was negligible. Practitioners are cautioned against using certain existing methods because the degree to which they over- or underestimate the likelihood of failure depended on the amount and location of decay in the cross-section.

Keywords Tree decay · Strength loss · Oscillation · Oak · Wind · Winching

Communicated by T. Fourcaud.

C. Ciftci (✉)
Department of Civil Engineering, Abdullah Gul University, Kayseri, Turkey
e-mail: cihan.ciftci@agu.edu.tr

B. Kane
Department of Environmental Conservation, University of Massachusetts, Amherst, MA, USA

S. F. Brena · S. R. Arwade
Department of Civil and Environmental Engineering, University of Massachusetts, Amherst, MA, USA

Introduction

Tree risk assessment is an important aspect of arboricultural practice. Tree failures regularly damage property and injure people. From 1995 to 2007, 407 people died in the US as a result of wind-related tree failures (Schmidlin 2009), although the presence of defects prior to tree failure was not assessed. There is also a risk of litigation associated with tree failures (Mortimer and Kane 2004), so the economic cost may be much greater than the direct cost of tree and debris removal and associated damage repair. Examples can be found in most cities: a recent series of articles in the New York Times detailed multiple lawsuits stemming from fatalities and injuries associated with hazardous trees (Glaberson and Foderado 2012).

The risk of tree failure due to decay may be quantified through different techniques that range from simple visual inspection (Fink 2009) to sophisticated decay detection

methods involving tomography (Gilbert and Smiley 2004; Nicolotti et al. 2003; Wang and Allison 2008), radar (Butnor et al. 2009), or tree performance measurements using strain gages and inclinometers (Sinn and Wessolly 1989). Assessing decay has been the focus of much research, primarily in the form of decay detection devices (Johnstone et al. 2010). Quantifying the amount of decay has been related to the probability of failure using strength loss formulas (Coder 1989; Mattheck et al. 1993; Smiley and Fraedrich 1992; Wagener 1963). Kane et al. (2001) reviewed the formulas and found that all are based on the moment of inertia (I) of a circular cross-section [excepting Mattheck et al. (1993)], and have been calibrated using empirical evidence. It should be noted that the level of sophistication and the quantity of investigations of testing of devices to detect decay far exceed the sophistication, accuracy and quantity of investigations of the strength loss formulas.

Wagener (1963) determined strength loss of a stem by dividing the cube of diameter of a, presumed, circular area of decay by the cube of the stem diameter (also assumed to be circular). This is a more conservative estimate of the loss in I of a circular cross-section due to a concentric, circular area of decay, which was Coder's (1989) approach. He estimated strength loss as the ratio of the diameter of a circular area of decay raised to the fourth power and the stem diameter raised to the fourth power. Wagener (1963) used a more conservative estimate of the loss in I given the limitations of the procedure. Limitations include: (1) neither stem cross-sections nor areas of decay are always perfectly circular; (2) bark thickness is not considered; (3) trees are not equivalent to defect-free specimens used to determine wood properties—slope of grain, reaction wood, juvenile wood, and branches (knots) are part of the tree; and (4) genetics and growing conditions contribute to variation in wood properties among individuals of a species.

Despite Wagener's (1963) more conservative assessment of the loss in I, additional limitations undermine the accuracy of the formulas. Primary among these is that the formulas do not explicitly consider the location of decay relative to the neutral axis and the distance between the neutral axis and the location of the maximum bending-induced normal stress (σ). The latter is related to the applied moment using the flexure formula for elastic materials that remain below the proportional limit:

$$\sigma = Mc/I \quad (1)$$

where M is the bending moment and c is the maximum perpendicular distance from the neutral axis to the outer surface of the branch or stem. Non-concentric areas of decay reduced the accuracy of Wagener's (1963) and Coder's (1989) formulas to predict strength loss (Kane and Ryan 2004) and breaking strength (Ruel et al. 2010) of stems. Stresses associated with axial forces are typically ignored when investigating strength loss because their magnitude is small as compared to bending stress (Mattheck et al. 1994).

A second limitation of the strength loss formulas is that they assume a homogeneous and isotropic material where tensile and compressive stresses depend on the same modulus of elasticity. Although conventional sources usually provide a single value for the modulus of elasticity (E) of wood in bending (e.g., Kretschmann 2010), some work has shown that E is greater in tension (E_T) than in compression (E_C) (Langum et al. 2009; Langwig et al. 1968; Ozyhar et al. 2013; Schneider et al. 1990). Consequently, the strain and stress distributions, under the classical assumptions of beam theory, will not be proportional to one another. Since E applies only to strains in the elastic range well below yield stress, an alternative value of E could be determined as the secant of a stress–strain curve including the non-linear region of plastic strains preceding rupture. Since wood is stronger in tension than compression (Bodig and Jayne 1993), in the region of non-linear strains, E determined from the secant would reflect difference between tensile and compressive values.

Finally, none of the formulas considers growth stresses, which are tensile at the periphery of the stem and compressive at the pith. Growth stresses can vary greatly among individuals of a given species (Jullien et al. 2013) and are greater on leaning stems due to the presence of reaction wood (Okuyama et al. 1994; Wilson and Gartner 1996; Yoshida et al. 2002). Depending on the particular conditions, the effect of growth stress may supersede any effect due to differences in E_T and E_C.

The objective of this paper is to improve predictions of MCL that account for areas of decay that vary with respect to size and distance from the perimeter of the cross-section, as well as those of irregular shapes. A secondary objective is to investigate whether the magnitude of disparity between the tensile and compressive elastic moduli of wood affected the reliability of the predictions.

Materials and methods

In deriving the improved predictions of MCL, several assumptions have been made. First, it was assumed that the stem or branch is subjected to pure bending stress; the effects of axial, shear and torsional stresses have been ignored. The reasons for this assumption were that wind-induced tree failures typically involve bending stress due to tree sway (James 2003) and experimental verification of the improved predictions involved primarily bending stress. Second, cross-sectional areas of the stem and decay

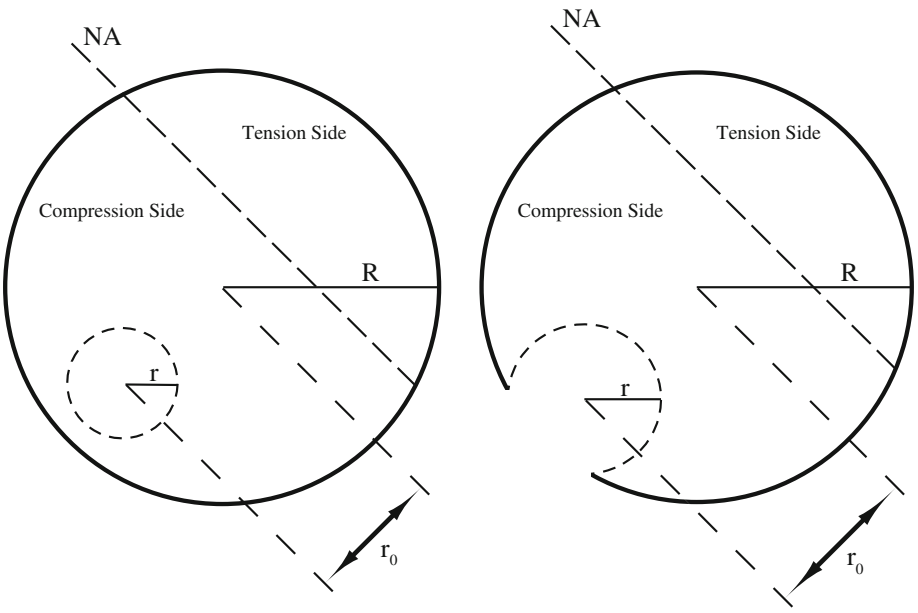

Fig. 1 Decay definition in tree cross-sections. The circle of radius *r*, outlined with a *dashed line*, indicates an area of decay. The left-hand figure is an example for a cavity completely contained within the tree cross-section and the right-hand figure is an example of a cavity that has breached the perimeter of the cross-section. The neutral axis, NA (where there are no bending strains) is the *dashed straight line* that separates the tension and the compression sides of the cross-sections. All *symbols* are explained in "Appendix A"

were assumed to be circular and defined by radii R and r, respectively, as shown in Fig. 1. The area of decay, still considered to be circular for simplicity, can also have an open cavity as in the right-hand side of Fig. 1. Third, the derivation assumes that the bending moment is applied on the plane whose intersection with the cross-section defines the line along a diameter that passes through the center of both the area of decay and the cross-section of the stem (Fig. 1). This assumption results in the maximum MCL of the cross-section, reflecting the greatest increase in likelihood of failure. Fourth, it has been assumed that: (a) $E_T > (E_C)$ (Langum et al. 2009), and (b) moment capacity is governed by compressive yield stress (Bodig and Jayne 1993), which is one-half that of tensile yield stress (Mattheck et al. 1994) and therefore defines the initiation of the failure process even though final apparent failure of the stem will manifest as tensile fracture. Lastly, the effect of growth stresses has been ignored. Previous studies have shown axial tensile growth stress in oaks of about 6 MPa (Okuyama et al. 1994; Wilhelmy and Kubler 1973; Yao 1979).

Definition of circular decay in tree cross-sections

The distance, r_0 in Fig. 1 defines the distance parallel to the diameter between the centers of the circular areas representing decay and the stem (Fig. 1). The ratio r_0/R will be used to evaluate the effect of decay position on MCL.

Theoretical approach and implementation

Moment capacity of the stem cross-section (with and without decay) can be calculated as the total moment of compressive and tensile stress resultants about the neutral axis of the cross-section. Thus, the first step in calculating moment capacity of stems with and without decay is to determine the location of the neutral axis. Figure 2 shows a representative stem cross-section with decay, as well as distributions of compressive and tensile strains and stresses (including the resultant compressive (F_C) and tensile (F_T) forces induced by bending). By definition, the neutral axis is located where bending strains are zero; it defines the transition between compressive (ε_C) and tensile (ε_T) strains. Because the section is subjected to pure bending, axial force equilibrium requires that $F_C = F_T$.

The location of the neutral axis coincides with the centroidal axis of the cross-section of the stem only for a section made from a homogeneous material that has symmetrical stress–strain response for both tension (E_T) and compression (E_C). That is, when

$$n = E_T / E_C = 1 \quad (2)$$

By defining the modular ratio n and transforming the cross-section to an equivalent homogeneous material, the neutral axis can be determined following basic principles of strength of materials. The main difficulty lies in an accurate determination of E_T and E_C. Such values are sparse in the literature (Langum et al. 2009), and vary by species and growing conditions (Bodig and Jayne 1993). Schneider and Phillips (1991) note that there is no reason to expect that E_T and E_C should be equal. If $n = 1$, MCL can be determined analytically for areas of decay located entirely within the cross-section of a stem ("Appendix B").

The effect of the location of the neutral axis on MCL was investigated by using two different values of n (1.1 and 2.0). For $n > 1.0$, the neutral axis will be closer to the

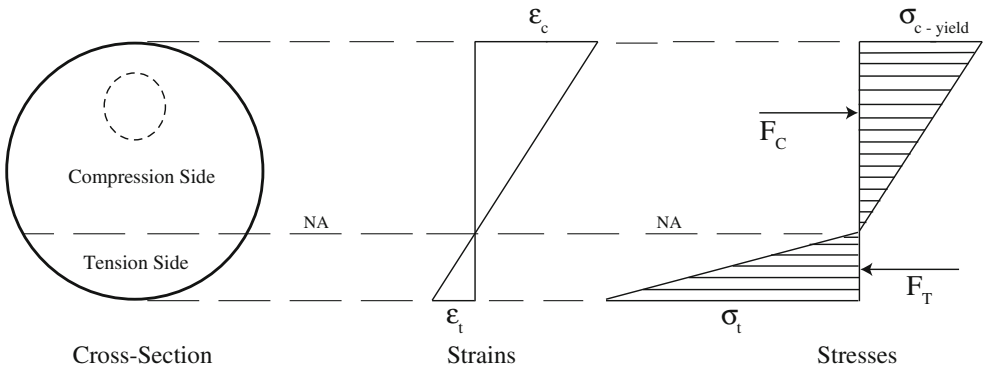

Fig. 2 Strains and stresses in compression and tension sides of tree cross-sections. The neutral axis, NA (where there are no bending strains) is the *dashed straight line* that separates the tension and the compression sides of the cross-sections. Axial stress due to self-weight and growth stresses have been ignored. All *symbols* are explained in "Appendix A"

tension side of the cross-section, so greater strains are generated on the compressive side where F_C acts. (Langum et al. 2009) presented values for young Douglas-fir (*Pseudotsuga menziesii* (Mirb.) Franco) and western hemlock (*Tsuga heterophylla* (Raf.) Sarg.); the mean value of n was approximately 1.1 ($E_C = 9{,}750$ MPa and $E_T = 10{,}400$ MPa). To determine whether the value of n affected MCL, $n = 2.0$ was also tested. These values covered the range of previously reported values of n (Langum et al. 2009; Langwig et al. 1968; Ozyhar et al. 2013; Schneider et al. 1990). Figure 2 shows that n dictates the proportional disparity between similar triangles representing ε_T and ε_C. For a given strain distribution, a stress distribution can be calculated (Fig. 2). The neutral axis was initially assumed to be at 1 % of the diameter of the cross-section, an unrealistically small value. Tensile and compressive strains that resulted from the assumed position of the neutral axis at each value of n were used to calculate σ_C and σ_T using Hooke's Law, assuming linear behavior of the material:

$$\sigma_i = E_i \varepsilon_i \tag{3}$$

where i designates compressive or tensile values of each parameter. From the distributions of compressive (σ_C) and tensile (σ_T) stresses, the resultant forces (F_C and F_T) were calculated by integrating σ_C and σ_T over the cross-sectional areas (Fig. 2). For each value of n, the preceding steps were repeated after gradually increasing the distance between the neutral axis and outer tension face of the stem in Fig. 1 until force equilibrium ($F_C = F_T$) was satisfied.

Once the location of the neutral axis of the tree cross-sections with and without decay was known, the moments of F_C and F_T about the neutral axis were calculated. Moment capacity of each section was defined as the total moment that generated a compressive stress in the extreme fiber equal to the compressive yield stress [taken from Kretschmann (2010)]. MCL due to decay was calculated:

Table 1 Morphometric data for ten red oaks tested to validate theoretical calculations of moment capacity loss

Parameter	Mean	SD
DBH (cm)	41	4.3
Tree height (m)	21.6	1.2
Crown width (m)[a]	11.9	2.3
Height of block (m)	13.8	1.3
Height of first branch (m)	10.3	2.1
Stem diameter at block (cm)	18	1.8
Angle between cable and tree (°)	73	2.5
% Of diameter notched (Type 1)	40	8.0
% Of diameter notched (Type 2)	12	6.0

[a] Calculated as the mean of widths measured parallel and normal to the direction of applied load

$$\mathrm{MCL} = 1 - \frac{\mathrm{MC_d}}{\mathrm{MC_{ud}}} \tag{4}$$

where MC_d and MC_{ud} are the moment capacities of the decayed and un-decayed sections, respectively.

Experiments on MCL

To validate the predictions of MCL for different amounts and locations of decay, ten red oaks (*Quercus rubra* L.) growing in Pelham, MA, USA (USDA Hardiness Zone 5A) were tested. Morphometric data of the trees are presented in Table 1. A static pull test similar to those summarized by (Peltola 2006) was used to test the trees. To limit the effect of the offset mass of the crown during testing, branches were removed prior to testing. A snatch block (McKissick Light Champion model 419) was attached to the tree with an Ultrex sling (1.9 cm diameter, Yale Cordage, Saco, ME) at approximately 65 % of its height. Trees were pulled using a skidder (John Deere model 440D) with a hydraulic winch and 61 m of Vectrus (1.3 cm diameter, Yale Cordage, Saco, ME). The rope was passed

Fig. 3 Two different types of notch were applied to tree stems. The direction of loading for the Type 1 notches was into the page; for Type 2 notches it was right to left

through the block and attached to a load cell (Dillon EDXtreme, Weigh-Tronix, Fairmont, MN) that recorded loads (accurate to 44 N) at 10 Hz. Loads were doubled, which was an overestimate because there was some amount of friction in the block, but this was assumed to be minor. Loads were resolved into components parallel and normal to the long axis of the trunk. Taking the sine of the mean angle between the applied force and the tree (Table 1) indicated that 96 % of the load was applied normal to the long axis of the trunk and induced a bending moment.

A strain meter was attached to the tension side of the stem approximately 1 m above ground as described by James and Kane (2008), which recorded axial displacements, which were converted to strains, at 20 Hz. To relate displacements with loads, the mean of two displacements was related with a single load for each 0.1 s. Trees were winched to induce axial displacements at the height of the strain meter of approximately 1–2 mm to ensure that induced stresses remained in the elastic range. The rate of loading varied with trees of different dimensions and time in the test (initial rates were less). Loading rate ranged from approximately 100–200 N/s, which induced displacements at a rate of approximately 0.1–0.2 mm/s.

After winching, a notch with its longitudinal axis normal to the direction of winching and the longitudinal axis of the trunk was cut into each tree with a chainsaw. Two types of notches were cut: (1) into the tension face of the trunk, removing all of the wood on the perimeter of the stem (two tests); (2) through the tree leaving wood intact at the perimeter of the trunk on the tension and compression faces (eight tests) (Fig. 3). More Type 2 notches were cut because of the variability of the location of the notch relative to the center of the trunk (as measured incident with the applied load). Three Type 2 notches left approximately equal thicknesses of wood on the proximal and distal sides of the trunk (relative to the position of the skidder); two left a greater thickness of wood on the proximal side of the trunk; and five left a greater thickness of wood on the distal

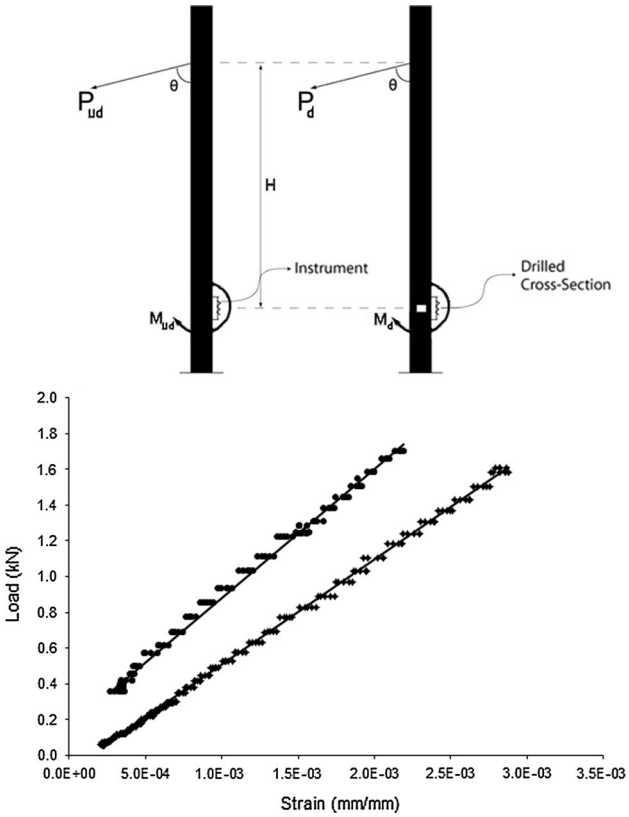

Fig. 4 Representation of the field experiments on the trees (defined in "Experiments on MCL") (*top*) and an example of a force–strain plot before (*filled circle*) and after (*filled dymond*) notching (*bottom*). All *symbols* are explained in "Appendix A"

side of the trunk. The mean percent of trunk diameter removed for each type of notch is included in Table 1.

Bending force was plotted against strain before and after the notch was cut on each tree. The slopes of the best-fit lines in Fig. 4 [before (k_{ud}) and after (k_d) notching] are related to the moment capacity of the tree as shown in the derivation of Eq. (16), which follows.

It should be noted that the theory developed in "Definition of circular decay in tree cross-sections" considered

circular areas of decay, but field tests described in "Experiments on MCL" treated non-circular areas of decay (Fig. 3), which, in cross-section were trapezoidal. It was impractical to create circular areas of decay in the field tests. Because of this limitation and the measurement of tensile rather than compressive axial strain, validation of the theory developed in "Definition of circular decay in tree cross-sections" considered loss in section modulus and trapezoidal areas of decay. After validating the theoretical approach, results will describe MCL, which is relevant to assessing the likelihood of failure due to decay.

Analysis of experimental data

In the following derivation, the subscripts (ud) and (d) refer to conditions before and after notching, respectively, and it was assumed that

$$E_{\mathrm{ud}} = E_{\mathrm{d}} \tag{5}$$

that is, notching does not alter the elastic moduli of the wood.

Hooke's Law can therefore be used to relate stress to strain at a particular point in the tree before and after notching:

$$\frac{\sigma_{\mathrm{ud}}}{\varepsilon_{\mathrm{ud}}} = \frac{\sigma_{\mathrm{d}}}{\varepsilon_{\mathrm{d}}} \tag{6}$$

Eq. (6) can be solved for σ_i:

$$\sigma_{\mathrm{ud}} = \frac{\varepsilon_{\mathrm{ud}}\sigma_{\mathrm{d}}}{\varepsilon_{\mathrm{d}}} \tag{7}$$

To find moments (M) of the applied force (P), the distance between the strain meter and the block on the tree (H) and θ (Fig. 4) must be known:

$$M_x = HP_x \sin\theta;\ x = \ \mathrm{ud},\ \mathrm{d} \tag{8}$$

where P_{ud} and P_{d} can be found for each tree as shown in Fig. 4:

$$P_x = k_x\varepsilon_x;\ x = \ \mathrm{ud},\ \mathrm{d} \tag{9}$$

and substituted into Eq. (8):

$$M_x = Hk_x\varepsilon_x \sin\theta;\ x = \ \mathrm{ud},\ \mathrm{d} \tag{10}$$

Eq. (1) can be re-written including n:

$$\sigma_x = n\frac{M_x c_x}{I_x};\ x = \ \mathrm{ud},\ \mathrm{d} \tag{11}$$

and values of M_{ud} and M_{d} from Eq. (10) can be substituted into Eq. (11):

$$x = \ \mathrm{ud},\ \mathrm{d}. \tag{12}$$

The section modulus (S) is calculated for two conditions before and after notching, respectively:

$$S_{\mathrm{ud}} = \frac{I_{\mathrm{ud}}}{C_{\mathrm{ud}}} = \frac{nHk_{\mathrm{ud}}\varepsilon_{\mathrm{ud}} \sin\theta}{\sigma_{\mathrm{ud}}} \tag{13}$$

$$S_{\mathrm{d}} = \frac{I_{\mathrm{d}}}{C_{\mathrm{d}}} = \frac{nHk_{\mathrm{d}}\varepsilon_{\mathrm{d}} \sin\theta}{\sigma_{\mathrm{d}}} \tag{14}$$

Substituting σ_{ud} from Eq. (7) into Eq. (13) yields:

$$S_{\mathrm{ud}} = \frac{nHk_{\mathrm{ud}}\varepsilon_{\mathrm{d}} \sin\theta}{\sigma_{\mathrm{d}}} \tag{15}$$

Since tensile strains were measured in field tests, it was inappropriate to compare the tests with theoretically determined MCL, which was based on compressive yield stress. To verify the approach described in "Theoretical approach and implementation", loss in section modulus ($\mathrm{LOSS_S}$) of the tension side of tested trees due to notching was calculated from values of k_{ud} and k_{d}:

$$\mathrm{LOSS_s} = 1 - \frac{S_{\mathrm{d}}}{S_{\mathrm{ud}}} = 1 - \frac{\frac{nHk_{\mathrm{d}}\varepsilon_{\mathrm{d}} \sin\theta}{\sigma_{\mathrm{d}}}}{\frac{nHk_{\mathrm{d}}\varepsilon_{\mathrm{d}} \sin\theta}{\sigma_{\mathrm{d}}}} = 1 - \frac{k_{\mathrm{d}}}{k_{\mathrm{ud}}}. \tag{16}$$

$\mathrm{LOSS_S}$ in the tension side of cross-sections of trees tested in situ was also determined as described in "Theoretical approach and implementation", except that areas of notches were considered trapezoidal instead of circular, consistent with Figs. 3, 5. For each value of r_0/R measured after notches were cut into trees, the disparity between empirically and theoretically determined $\mathrm{LOSS_S}$ values was plotted for both values of n. (For trapezoidal areas cut into trees, r_0 represents the height of the trapezoid.)

Results and discussion

Comparison of the theoretical MCL with the experimental results

Figure 6 illustrates the difference between empirical values and theoretical predictions of $\mathrm{LOSS_S}$. For a range of $-0.10 < r_0/R < 0.13$, the maximum disparity between empirically and theoretically determined $\mathrm{LOSS_S}$ was <10 %, nor was the magnitude of disparity related to r_0/R: (a) disparities of equal magnitude occurred at several values of r_0/R and (b) the disparities were not similar for three trees with the same value of r_0/R (0.01). These results suggest that differences were random rather than systematic. Differences were presumably due to assumptions used to derive the theoretical values of $\mathrm{LOSS_S}$ such as perfect circular and trapezoidal areas for stem and area of decay, respectively, and homogenous material properties within the compression and tension sides of the stem. Ignoring the effect of growth stress may be another source of error.

Measurement error may have also contributed to the observed differences. Diameter of trees was measured

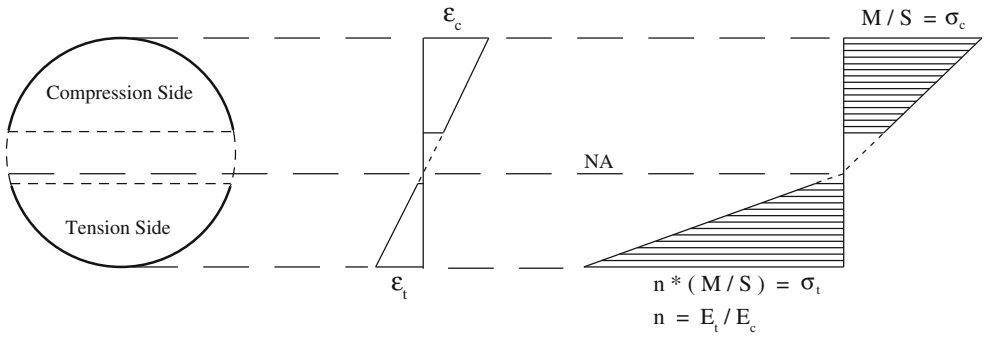

Fig. 5 Strains and stresses in compression and tension sides of tree cross-section with Type 2 notches described in "Experiments on MCL". Type 2 notches are represented by the *dashed closed* nearly *trapezoidal area* in the tree cross-section. The neutral axis, NA (where there are no bending strains) is the *dashed straight line* that separates the tension and the compression sides of the cross-sections. All *symbols* are explained in "Appendix A"

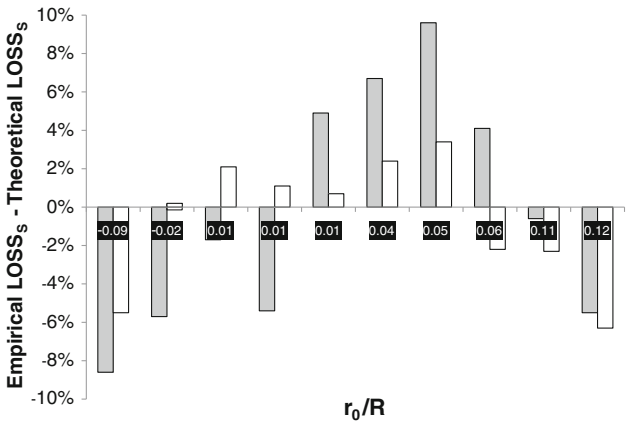

Fig. 6 Disparity between empirically and theoretically determined $LOSS_S$ for the stems of ten red oaks plotted according to the measured value of r_0/R after cutting a notch through the stem. Columns represent the disparity calculated for $n = 1.1$ (*shaded*) and $n = 2.0$. Two trees had Type 1 notches ($r_0/R = 0.11$ and 0.12); the remaining trees had Type 2 notches. *Symbols* are explained in "Appendix A"

outside the bark, and it was assumed that (a) bark thickness was 2 cm for all trees, and (b) bark was assigned a null value for *E*. From a practical standpoint, the greatest difference is important because it reflects the degree to which an assessor might over- or underestimate MCL of a tree. Using $n = 1.10$, the two greatest differences of 8.6 and 9.8 % were nearly twice that of the two greatest differences obtained using $n = 2.00$ (Fig. 6). The standard deviation of the differences was also greater when using $n = 1.10$ when compared with $n = 2.00$ (Fig. 6). For the red oaks tested, the model predictions agree more closely when $n = 2.00$ is used in the calculation rather than $n = 1.10$. This indicates a possible greater asymmetry in the elastic moduli of red oak than Douglas-fir, but it was not possible to investigate further since growth stress was not accounted for.

Effect of area and location of decay

Figure 7 shows MCL of the cross-section of a tree relative to size and location of decay in the cross-section. Only values of $r_0/R \geq 0$ have been included in Fig. 7 since compressive yield stress was used to define moment capacity. Consequently, MCL for $r_0/R \geq 0$ is greater than for $r_0/R < 0$ (Fig. 8). In Fig. 7, it has been assumed that $n = E_t/E_c = 1.10$ [consistent with Langum et al. (2009)]. To describe the location of decay, the ratio r_0/R was used as illustrated in Fig. 1. Linear interpolation may be used for values of r_0/R not included in Fig. 7. For $r_0/R = 0.40$, for example, MCL can be interpolated between the curves for $r_0/R = 0.33$ and 0.50.

Inflection points of the curves for various r_0/R ratios in Fig. 7 correspond to the formation of an open cavity of decay in the cross-section, i.e., when,

$$r + r_0 = R \tag{17}$$

The interaction of size (r/R) and location (r_0/R) is underscored by Fig. 7. For example, a specific size of decay ($r/R = 0.5$) can have varying MCL values depending on location: 7 % for $r_0/R = 0.00$ (concentric decay), 28 % for $r_0/R = 1.00$, and 49 % for $r_0/R = 0.50$. A similar pattern exists for other values of r/R, although the magnitude of disparity decreases as r/R approaches zero. A careless accounting for the location of decay could grossly under- or overestimate MCL of the stem, even for relatively small areas of decay. As an example, Wagener (1963) suggested that when the diameter of an area of decay was 70 % of the diameter of the cross-section there was a greater likelihood of failure. Figure 7 shows that MCL at $r/R = 0.7$ can be quite variable depending on decay location. Conversely, MCL of 0.30 occurs at very different values of r/R, depending on the value of r_0/R.

Figure 9 compares Wagener's (1963) and Coder's (1989) predictions of strength loss, which assume $n = 1.0$

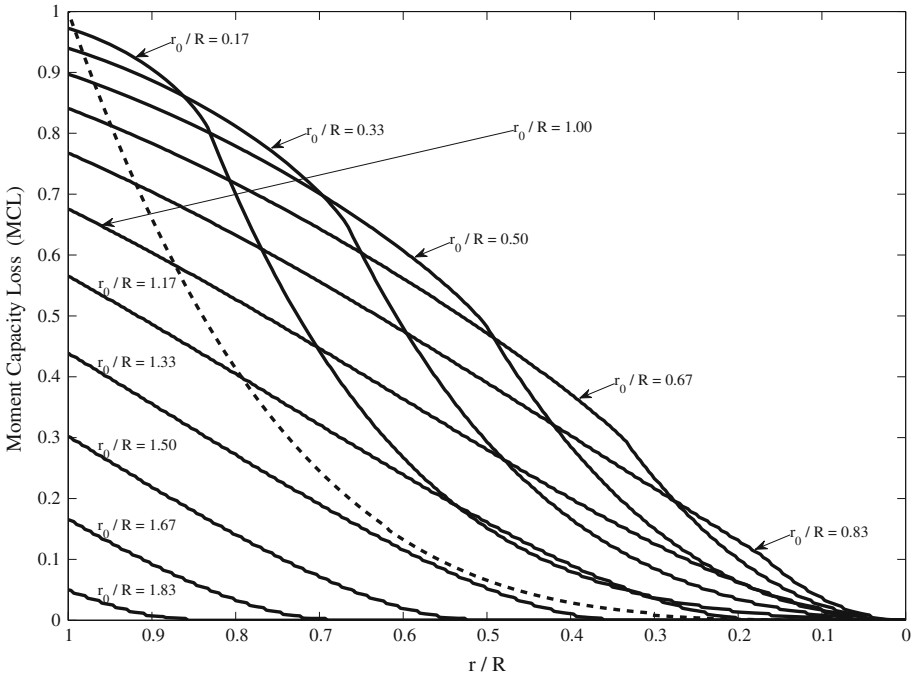

Fig. 7 Moment capacity loss values for different sizes (r/R) and different locations (r_0/R) of decay ($n = 1.10$). The *dashed line* refers to $r_0/R = 0$, the case of concentric decay. Only values of $r_0/R > 0$ are shown since decay in the compression side causes greater moment capacity loss and it is conservative to assume that the wind direction is such that the decay is in the compression side (see Fig. 8)

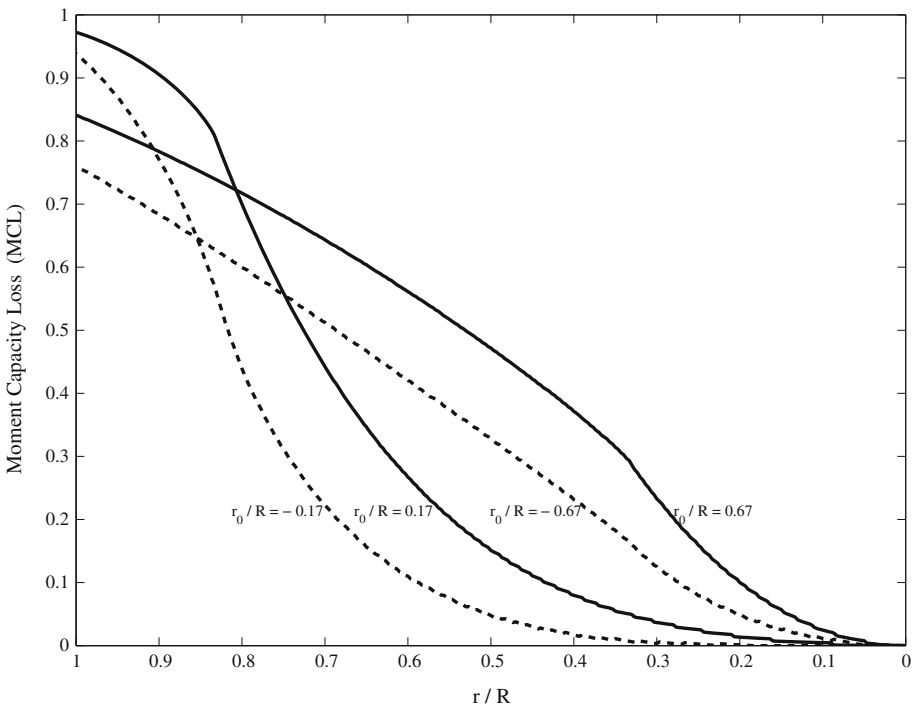

Fig. 8 Moment capacity loss values for different sizes (r/R) and different locations (r_0/R) of decay ($n = 1.10$). *Dashed lines* refer to $r_0/R < 0$, the case of decay on the side of the cross-section undergoing tensile bending stress. *Solid lines* refer to $r_0/R > 0$, the case of decay on the side of the cross-section undergoing compressive bending stress

and decay is concentric, with prediction of MCL for concentric decay and $n = 1.10$ (which is the dashed line in Fig. 7). As expected, there is only a small difference between Coder's (1989) formula, because MCL of concentric decay assuming $n = 1.00$ is simply the ratio of the moments of inertia of decay to cross-section of the tree ("Appendix B"). Since Wagener's (1963) formula is the ratio of the cubes of the diameters of decay to that of the cross-section of the tree, it predicts greater MCL for each value of r/R. Smiley and Fraedrich's (1992) formula is the same as Wagener's (1963) when no cavity is present. Referring to Fig. 7, however, it is easy to see how poorly each of the formulas accounts for areas of decay that are entirely within the cross-section, but not

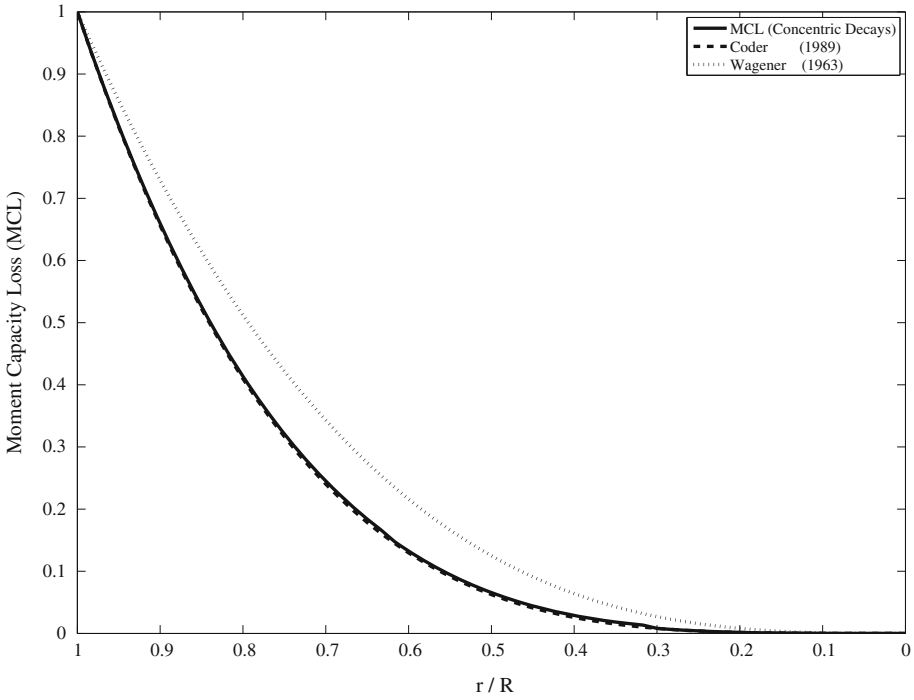

Fig. 9 Comparison of MCL for concentric decay (assuming $n = 1.10$) with predictions of loss in moment of inertia according to Coder (1989) and Wagener (1963)

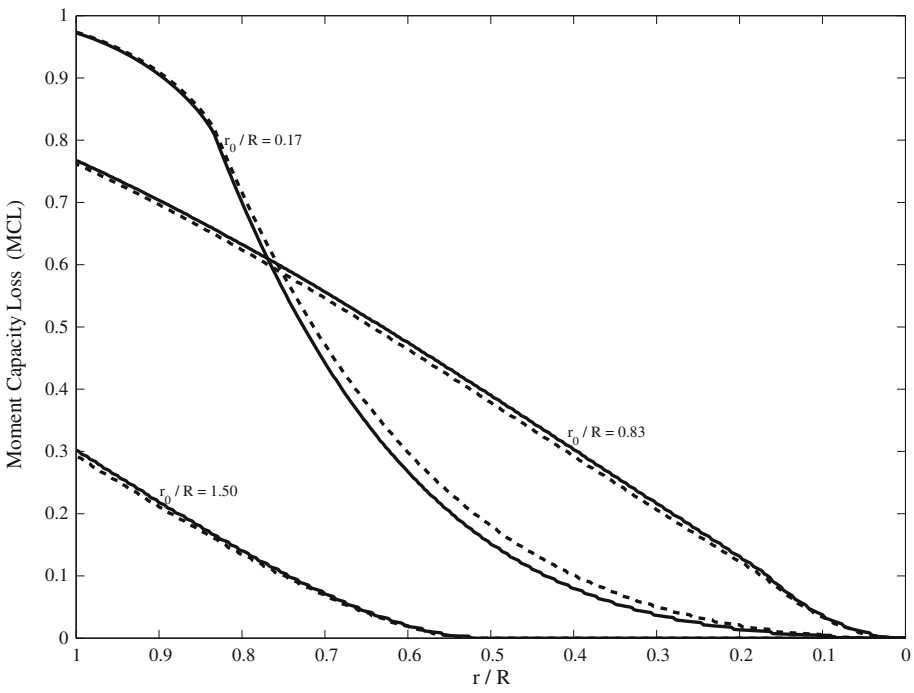

Fig. 10 Effect of n (1.1, 2.0) on moment capacity loss for three values of r_0/R (0.17, 0.83, and 1.50). The *solid lines* represent $n = 1.1$, the *dashed lines* indicate $n = 2.0$

concentric (i.e., $0 < r_0/R < 1$). Such disparities are particularly important because the formulas have action thresholds. For example, Wagener (1963) suggested that conifers were more likely to fail when strength loss exceeded 33 %; using his formula, this threshold occurs at $r/R = 0.70$. MCL of 35 %, however, occurs between $0.35 < r/R < 0.90$. Similarly, Coder (1989) described the "caution zone" when strength loss exceeded 20 %, which occurs at $r/R \approx 0.66$. MCL of 0.20, however, occurs between $0.25 < r/R < 0.70$, depending on the value of r_0/R (Fig. 7). In light of such disparities, these formulas should not be used to assess the likelihood of failure due to decay, consistent with previous findings (Kane and Ryan 2004).

Effects of modular ratio (n) on MCL

Figure 10 shows that different values of n would not dramatically change MCL of decayed sections. The small effect of n on MCL suggests that Fig. 7 should apply to a wide range of species and growing conditions. However, not accounting for growth stress would make predictions of MCL less applicable on trees where growth stresses were expected to be large (e.g., trees with reaction wood due to leaning stems).

Assessment of decay shape on MCL

Although decay in trees can sometimes adopt an approximately circular or other areas with simple geometry, decay mostly forms irregular shapes (Shigo 1984) and the extent of decay can vary by tree species and presence of fungus (Deflorio et al. 2008). Two methods can be used to estimate MCL of such decayed stems using the curves developed in this paper. The first method can be used without excessive calculations, making it suitable for use in the field. The second method requires a more careful accounting of the area and location of decay.

Method I

An irregularly shaped area of decay can inscribe and be inscribed by circles. Figure 11 shows a rectangular area of decay, but this method can be applied to areas of any shape. MCL can be determined from Fig. 7, assuming r and r_0 from the smaller and larger circles inscribed or inscribing the decay area. Practitioners could compare three estimates of MCL: using the larger circle, the smaller circle, or a mean value. Depending on the loading conditions (sheltered or exposed trees, for example) or other factors related to risk assessment (such as value of the target), conservative or lenient estimates of MCL could be employed. This approach may offer an advantage over the method described by Mattheck et al. (1993), who suggested using the thinnest remaining wall of sound wood when assessing off-center areas of decay, which tended to overestimate the loss in moment of inertia of such stems (Kane and Ryan 2004).

Method II

In this method, an irregularly shaped area of decay can be converted into a circle of equivalent area as in Fig. 12. In order for the method to be valid, the irregularly shaped area of decay and its circular equivalent must share the same centroid. After conversion to a circular area, MCL loss of the section can be determined from Fig. 7. For simple geometric shapes, like a rectangle, the methods will yield very similar results because it is easy to convert the areas into circles and determine the centroids. For irregularly shaped areas, determining the area and centroid requires more rigorous analysis and, likely, the use of image analysis software. For practitioners, images can be gleaned from tomography (Gilbert and Smiley 2004; Wang and Allison 2008), but this method requires sophisticated tools and techniques.

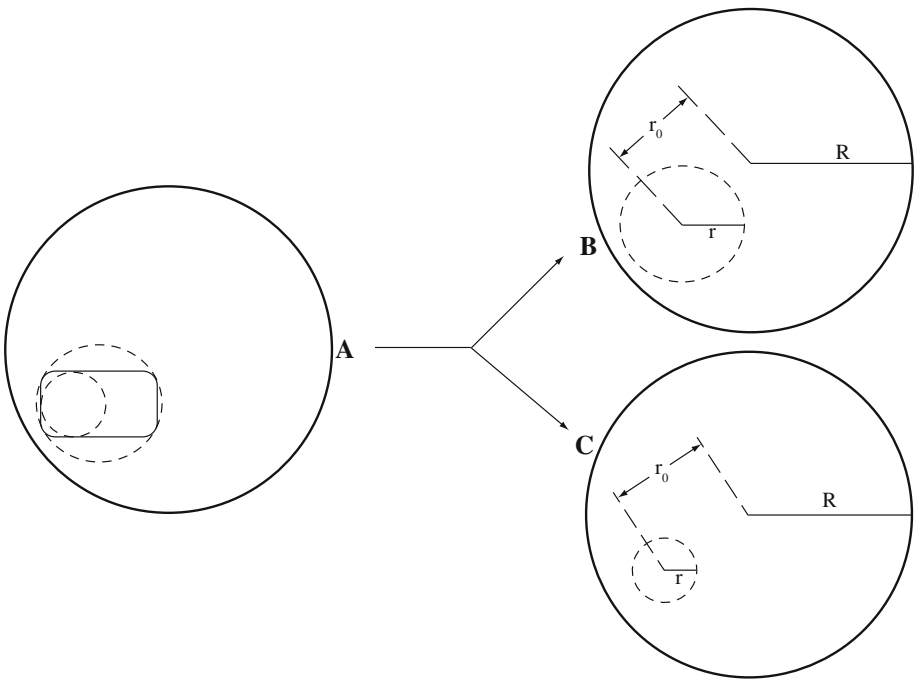

Fig. 11 Description of method I addressed in "Method I". As an example, a rectangular area of decay is shown in a *circular* tree cross-section (**a**). Figures **b** and **c** graphically depict how method I can be used to determine the upper limit and lower limit, respectively, of moment capacity loss of the rectangular area of decay. All *symbols* are described in "Appendix A"

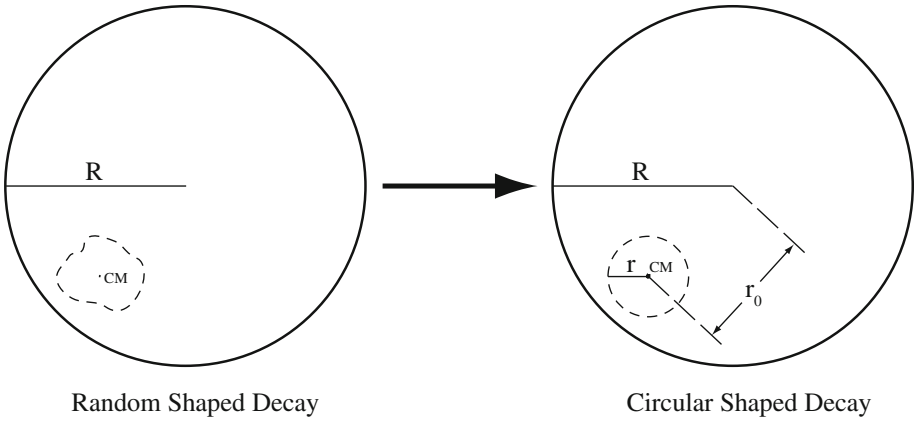

Fig. 12 Description of method II addressed in "Method II". The random area of decay is converted into a *circular* area. CM refers to the geometric center of the decay. Other *symbols* are described in "Appendix A"

Conclusions

The maximum MCL of any decayed cross-section of a tree without a noticeable lean can be approximated using methods I or II, and Fig. 7. Similarity between (a) theoretically and empirically determined values of $LOSS_S$ and (b) values of MCL calculated for a wide range of values of n lends confidence that these methods can be reasonably applied under a variety of field conditions. The effect of n on estimation of MCL was negligible. Practitioners should consider Fig. 6 to better understand the range of variation in MCL as affected by n. Four limitations regarding applicability of the MCL procedures described in the paper include: (1) not accounting for axial stresses induced by dead load and the vertical component of the pulling tests, (2) not accounting for growth stresses and other innate variations in wood properties (e.g., reaction wood), (3) altered E values of wood formed after wounding, and (4) presumption of the location of failure. The ratio of axial to bending stress during the tests was minimal (<0.1 %). The effect of growth stress may confound the analysis of MCL in practice because of the pre-stressed cross-section. This would especially apply to trees with leaning stems and reaction wood since the magnitude of growth stress would be greater (Archer 1987). Future studies should investigate this effect, especially considering that areas of decay will alter the cross-sectional distribution of growth stress. Regarding the third limitation, Kane and Ryan (2003) documented an increase in toughness of woundwood of red maple, which may also apply to E. Perhaps most importantly, practitioners must recognize that MCL due to decay ignores the possibility of failure at another location in the tree. Other defects (such as weak branch attachments or poor root anchorage) may fail prior to parts of the tree with decay. Thresholds for poor branch attachments (Kane 2007, Kane et al. 2008) and root loss (Smiley 2008) have been proposed.

The methods described in "Assessment of decay shape on MCL" provide estimates of the MCL (based on compressive yield stress) of a tree with decay. Although some of the wood of a tree may fail in compression when loaded, collapse and ultimate failure of the tree may not always coincide with compressive yield (Mattheck et al. 1994; Mergen 1954). Figure 7 thus provides a more conservative estimate of the likelihood of tree failure, which is preferable in the interest of avoiding injuries and property damage. To determine whether a threshold value of MCL existed and to further validate the predictions following the methods presented, failed and intact branches and stems with decay could be measured after a windstorm. Previous attempts to find a threshold (Mattheck et al. 1993, 1994) have been problematic (Fink 2009; Gruber 2008), so care must be taken in sampling and analyzing such data. With a reliable sample and normal distribution, the first and the second moments (mean and standard deviation) of the distribution can illustrate the MCL of different species under wind-induced bending.

Acknowledgments This study was funded by the TREE Fund's Mark S. McClure Biomechanics Fellowship. Nevin Gomez, Sherry Hu, Alex Julius, Dan Pepin, Alex Sherman, and Joseph Scharf (University of Massachusetts-Amherst) helped collect data.

Appendix A: Acronyms and abbreviations

c	Perpendicular distance from the neutral axis to a point whose tension or compression stress will be calculated
E_C	Wood compressive Young's modulus parallel to grain
E_T	Wood tensile Young's modulus parallel to grain
F_C	Resultant compressive force at the compression side in a stem cross-section
F_T	Resultant tensile force at the tension side in a stem cross-section
H	Height (see Fig. 4) between the puling force and the strain meter of the experiments described in "Experiments on MCL"

I Moment of inertia of a cross-sectional area computed about the neutral axis
k_d The slope of the curve in Fig. 4 after notching
k_{ud} The slope of the curve in Fig. 4 before notching
M Bending moment
M_d Calculated bending moment [Eq. (8)] for the experiments (after notching) described in "Experiments on MCL"
M_{ud} Calculated bending moment [Eq. (8)] for the experiments (before notching) described in "Experiments on MCL"
n Modular ratio of E_T to E_C
P_d Pulling force measures from the experiments (after notching) described in "Experiments on MCL"
P_{ud} Pulling force measures from the experiments (before notching) described in "Experiments on MCL"
r Radius of the circular decay defined in Fig. 1
r_0 Distance between the centers of the tree section and decayed area defined in Fig. 1
R Radius of the circular tree cross-section defined in Fig. 1
S Section modulus of tree cross-sections
ε_c Strain at the outer face of the compression side in a stem cross-section
ε_d Strain meter measures from the experiments (after notching) described in "Experiments on MCL"
ε_t Strain at the outer face of the tension side in a stem cross-section
ε_{ud} Strain meter measures from the experiments (before notching) described in "Experiments on MCL"
σ Bending stress
$\sigma_{c\text{-}yield}$ Yield compressive stress at the outer face of the compression side in a stem cross-section
σ_t Tensile stress at the outer face of the tension side in a stem cross-section
θ Angle (see Fig. 4) between the pulling force and the tree stem for the experiments described in "Experiments on MCL"

Appendix B: MCL for areas of decay confined within the cross-section

If $n = 1$, MCL of areas of decay confined within the cross-section can be determined from the ratio of the section modulus of the decay to that of the tree cross-section, assuming each is circular. To obtain the section moduli, first, the moments of inertia (I) for the tree cross-section and decay area are:

$$I = \frac{\pi}{4}R^4 \tag{18}$$

$$I_d = \frac{\pi}{4}r^4 \tag{19}$$

in which R and r are the radii of cross-section and the decayed area, respectively, and the subscript d indicates the area of decay. The areas (A) of these sections are:

$$A = \pi R^2 \tag{20}$$

$$A_d = \pi r^2 \tag{21}$$

To find the location of the neutral axis (ΔX) of the tree cross-section with decay:

$$\Delta X = \frac{A_d r_0}{A - A_d} \tag{22}$$

where r_0 refers to the distance between the centers of the tree section and decayed area. The moment of inertia of the hollow section (the tree cross-section with decay) (I_H) can be determined:

$$I_H = I - I_d + A(\Delta X)^2 - A_d(\Delta X + r_0)^2 \tag{23}$$

Then, the distance (c) between the circumference of tree cross-section and the neutral axis is:

$$c = R + \Delta X \tag{24}$$

Finally, loss of section modulus can be calculated as:

$$s_{loss} = \frac{I/R - {}^{I}H/c}{I/R} \tag{25}$$

References

Archer RR (1987) Growth stresses and strains in trees. Springer in wood science. Springer-Verlag, Berlin

Bodig J, Jayne BA (1993) Mechanics of wood and wood composites. Krieger Publishing Company, Malabar

Butnor JR, Pruyn ML, Shaw DC, Harmon ME, Mucciardi AN, Ryan MG (2009) Detecting defects in conifers with ground penetrating radar: applications and challenges. For Pathol 39:309–322

Coder KD (1989) Should you or shouldn't you fill tree hollows? Grounds Maint 24(9):68–70

Deflorio G, Johnson C, Fink S, Schwarze FWMR (2008) Decay development in living sapwood of coniferous and deciduous trees inoculated with six wood decay fungi. For Ecol Manage 255(7):2373–2383. doi:10.1016/j.foreco.2007.12.040

Fink S (2009) Hazard tree identification by visual tree assessment (Vta): scientifically solid and practically approved. Arboric J 32(3):139–155. doi:10.1080/03071375.2009.9747570

Gilbert EA, Smiley ET (2004) Picus sonic tomography for the quantification of decay in white oak (Quercus alba) and hickory (*Carya* spp.). J Arboric 30:277–281

Glaberson W, Foderado LW (2012) Neglected, rotting trees turn deadly. The New York Times, New York

Gruber F (2008) Reply to the response of Claus Mattheck and Klaus Bethge to my criticisms on untenable vta-failure criteria, who is right and who is wrong? Arboric J 31(4):277–296

James K (2003) Dynamic loadig of trees. J Arboric 29(3):165–171
James KR, Kane B (2008) Precision digital instruments to measure dynamic wind loads on trees during storms. J Arboric 148(6–7):1055–1061. doi:10.1016/j.agrformet.2008.02.003
Johnstone D, Tausz M, Moore G, Nicolas M (2010) Quantifying wood decay in Sydney Bluegum (Eucalyptus saligna) trees. Arvoric Urban For 36(6):243–252
Jullien D, Widmann R, Loup C, Thibaut B (2013) Relationship between tree morphology and growth stress in mature European beech stands. Ann For Sci 70(2):133–142. doi:10.1007/s13595-012-0247-7
Kane B (2007) Branch strength of Bradford pear (*Pyrus calleryana* var. 'Bradford'). Arboric Urban For 33(4):283–291
Kane B, Ryan D (2003) Examining formulas that assess strength loss due to decay in trees: woundwood toughness improvement in red maple (Acer rubrum). J Arboric 29(4):207–217
Kane B, Ryan D (2004) The accuracy of formulas used to assess strength loss due to decay in trees. J Arboric 30(6):347–356
Kane B, Ryan D, Bloniarz DV (2001) Comparing formulae that assess strength loss due to decay in trees. J Arboric 27(2):78–87
Kane B, Farrell R, Zedaker SM, Loferski JR, Smith DW (2008) Failure mode and prediction of the strength of branch attachments. Arboric Urban For 34(5):308–316
Kretschmann DE (2010) Mechanical properties of wood. In: Wood handbook, wood as an engineering material, vol 5. Department of Agriculture, Forest Service, Forest Products Laboratory, Madison, pp 1–46
Langum CE, Yadama V, Lowell EC (2009) Physical and mechanical properties of young-growth Douglas-fir and western hemlock from western Washington. For Prod J 59(11/12):37–47
Langwig JE, Meyer JA, Davidson RW (1968) Influence of polymer impregnation on mechanical properties of basswood. For Prod J 18(7):31–36
Mattheck C, Bethge K, Erb D (1993) Failure criteria for trees. Arboric J 17:201–209
Mattheck C, Lonsdale D, Breloer H (1994) The body language of trees: a handbook for failure analysis. HMSO, London
Mergen F (1954) Mechanical aspects of wind-breakage and wind-firmness. J For 52(2):119–125
Mortimer MJ, Kane B (2004) Hazard tree liability in the United States: uncertain risks for owners and professionals. Urban For Urban Green 2(3):159–165. doi:10.1078/1618-8667-00032
Nicolotti G, Socco LV, Martinis R, Godio A, Sambuelli L (2003) Application and comparison of three tomographic techniques for detection of decay in trees. J Arboric 29(2):66–78
Okuyama T, Yamamoto H, Yoshida M, Hattori Y, Archer R (1994) Growth stresses in tension wood: role of microfibrils and lignification. Ann For Sci 51(3):291–300
Ozyhar T, Hering S, Niemz P (2013) Moisture-dependent orthotropic tension-compression asymmetry of wood. Holzforschung, vol 67. doi:10.1515/hf-2012-0089
Peltola HM (2006) Mechanical stability of trees under static loads. Am J Bot 93(10):1501–1511. doi:10.3732/ajb.93.10.1501
Ruel J-C, Achim A, Herrera R, Cloutier A (2010) Relating mechanical strength at the stem level to values obtained from defect-free wood samples. Trees 24(6):1127–1135. doi:10.1007/s00468-010-0485-y
Schmidlin T (2009) Human fatalities from wind-related tree failures in the United States, 1995–2007. Nat Hazards 50(1):13–25. doi:10.1007/s11069-008-9314-7
Schneider MH, Phillips JG (1991) Elasticity of wood and wood polymer composites in tension compression and bending. Wood Sci Technol 25(5):361–364. doi:10.1007/BF00226175
Schneider MH, Phillips JG, Tingley DA, Brebner KI (1990) Mechanical properties of polymer-impregnated sugar maple. For Prod J 40(1):37–41
Shigo AL (1984) How to assess the defect status of a stand. North J Appl For 1(3):41–49
Sinn G, Wessolly L (1989) A contribution to the proper assessment of the strength and stability of trees. Arboric J 13:45–65
Smiley ET (2008) Root pruning and stability of young willow oak. Arboric Urban For 34(2):123–128
Smiley ET, Fraedrich BR (1992) Determining strength loss from decay. J Arboric 18(4):201–204
Wagener WW (1963) Judging hazard from native trees in California recreational areas: a guide for professional foresters. US Forest Service Research Paper, PSW-P1, p 29
Wang X, Allison RB (2008) Decay detection in red oak trees using a combination of visual inspection, acoustic testing, and resistance microdrilling. Arboric Urban For 34(1):1–4
Wilhelmy V, Kubler H (1973) Stresses and checks in log ends from relieved growth stresses. Wood Sci 6:136–142
Wilson BF, Gartner BL (1996) Lean in red alder (Alnus rubra): growth stress, tension wood, and righting response. Can J For Res 26(11):1951–1956
Yao J (1979) Relationships between height and growth stresses within and among white ash, water oak, and shagbark hickory. Wood Sci 11(4):246–251
Yoshida M, Ohta H, Okuyama T (2002) Tensile growth stress and lignin distribution in the cell walls of black locust (Robinia pseudoacacia). J Wood Sci 48(2):99–105. doi:10.1007/BF00767285